THREE-DIMENSIONAL FEM MODEL OF THE FATIGUE CRACK GROWTH IN A THICK CT SPECIMEN

V. OLIVA, A. MATERNA AND P. MICHLÍK

Department of Materials, Faculty of Nuclear Sci and Physical Engng, CTU in Prague
Trojanova 13, 120 00 Prague 2, Czech Republic

ABSTRACT

A 3D elastic-plastic finite element model with small strains was used for simulation of the behaviour of the growing fatigue crack. Through-thickness fatigue crack propagation in a thick CT specimen made of Al 7010 alloy and loaded by constant amplitude tension with high stress ratio was simulated. The influence of a free surface was found only in a very thin surface layer. Cyclic stresses and plastic strains correspond to the plane strain simulation at the nearly whole crack front. The state of stress at the ends of the straight crack front is similar to the plane stress, but local plastic strain range is low and comparable with plane strain simulation.

The results were used also for a direct estimation of the fatigue crack growth rate from local low-cycle fatigue conditions at the crack front. Such estimation based on plane stress simulation gives a good result for the crack in a thin-walled body. The estimation of the crack rate in a thick wall requires the knowledge of parameters of low-cycle fatigue under intensive restraint of plastic deformation. The critical strain energy density for such conditions will be probably substantially lower than the value resulting from the common low-cycle fatigue tests.

KEYWORDS

fatigue, fatigue crack modelling , crack propagation, crack closure, crack rate prediction

INTRODUCTION

The prediction of long through-thickness fatigue crack growth in thin-walled elements is a relatively well understood problem that may be solved by various computational algorithms based mostly on the stress intensity factor or its effective value. However, the simulation of surface cracks or through-thickness cracks growing in thick-walled parts with complicated geometry still remains an open question [1], [2]. In such three-dimensional cases difficulties may arise from an inexplicit definition of the local stress intensity at the part of the curved crack front near the free surface, from complicated crack closing, from the change of local out-of plane constraint along the crack front [3], from a different (tensile or shear) fracture mode in various parts of the crack surface, etc.

Elastic-plastic FEM simulations of fatigue crack behaviour were used many times to analyse the crack closing [4]. Two-dimensional models were used to predict the crack growth rate [5] and the crack behaviour under sudden changes of cyclic loading [6], [7]. In this paper we have attempted to give a FEM description of the cyclic stress and plastic deformation along the straight front of a through-crack in a thick wall. The results are used also for an attempt at a direct theoretical prediction of the crack growth rate from local low-cycle fatigue conditions immediately in front of the crack. We believe that such simulations can provide a useful insight into the three-dimensional fatigue crack problem, even though they can be used for studying only very short segments of the crack propagation.

FEM MODEL

Geometry and finite element mesh

A model problem was chosen to correspond to the experiments described in [8]. A through-thickness fatigue crack with a straight front grows in a CT specimen 25 mm thick (Fig.1) from the initial coordinate $x = 36.250$ mm to the position $x = 36.326$ mm. The final crack length is $a = 8.826$ mm.

One half of the specimen was covered by a 2D finite element mesh of elements, as shown in Fig. 1. The size of the smallest elements around the crack in the *(x,z)* plane was 0.004 mm. Finally the mesh was extruded to the centre plane of the specimen so that a 3D mesh with 5424 eight-noded elements with a 2 x 2 x 2 integration was created.

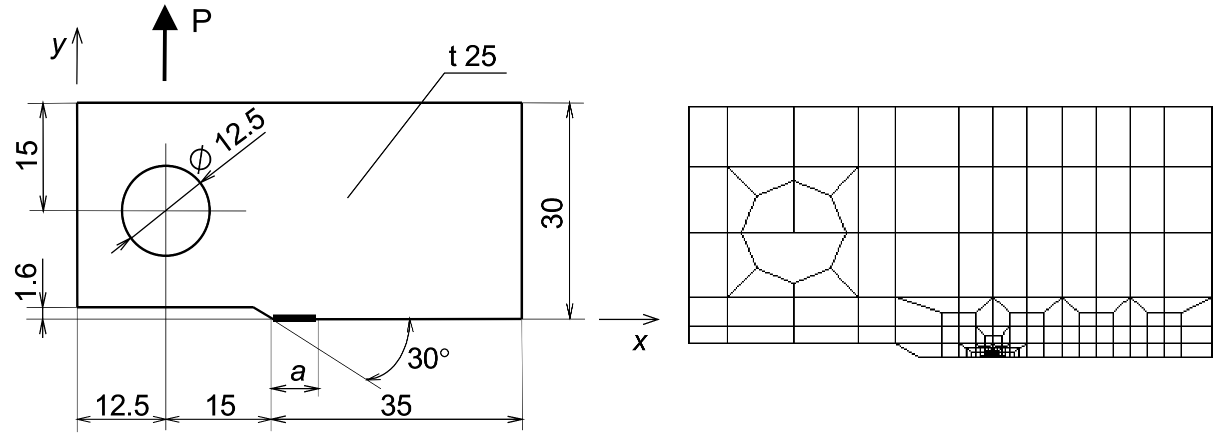

Fig. 1. Geometry of CT specimen and finite element mesh.

Material

The real CT specimen was made of Al7010 alloy (E = 67 900 MPa, μ = 0.34, 0.2% yield stress ~ 400 MPa). The input material data should reflect the cyclic hardening and the damage accumulation under cyclic plastic deformation; therefore the data were obtained from common low-cycle fatigue tests (tension-compression).

The stabilized stress-strain curve was obtained from the tensile test performed after previous intensive cyclic loading with a strain amplitude of 1 %. The curve had to be extrapolated to the strain of several tens of percent. Bauschinger effect influencing the shape of hysteresis loop was taken into account.

The low-cycle fatigue properties of the alloy were described by the parameters β, ε_c of Manson-Coffin relation $\Delta\varepsilon_p\, N_f^{\ \beta} = \varepsilon_c$ ($\Delta\varepsilon_p$ - plastic strain range, N_f - number of cycles to fracture) and by critical strain energy density to fracture λ_c, obtained as the sum of the hysteresis loop areas obtained from strain controlled fatigue tests.

Model loading, crack growth and finite element solution

Model sequence of the cyclic tensile loading with the high stress ratio $R = 0.7$ is shown schematically in Fig. 2. A total of 39 cycles was applied.

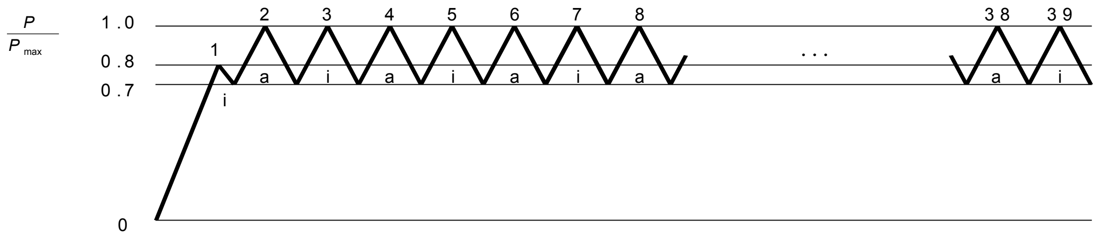

Fig. 2. Model cyclic loading and the fatigue crack growth.

The letter "a" denotes "active" cycles with a relatively large prescribed crack jump (4 μm) that is much longer than the real crack growth rate. Such large crack extension results in the unrealistically intensive plastic deformation during the cycle. To eliminate this shortcoming, an "idle" cycle without crack movement (letter "i") was inserted between each two active cycles. It is reasonable to suppose that crack front deformation mechanics in the idle cycle will be much closer to the situation in the real cycle with very small crack advance.

An elementary crack extension of the length of one element side was prescribed at the beginning of every active cycle. Such approach leads to a smooth development of the plastic deformation during the loading. The extension was simulated by releasing the nodes at the crack front.

In the first cycle, the CT specimen was loaded only up to 80 % of the maximum load P_{max}. This "trick" reduced the influence of the artificially high plastic deformation induced by the first model cycle and shortened the path necessary for stabilising the crack behaviour.

The FEM program MSC.Marc was used for modelling. The 2D and 3D numerical simulations can be briefly described as follows: small strain formulation, five or four load increments per a half-cycle, the Von Mises yield criterion, kinematic hardening rule, and possible contact of the crack surface with the (x,z) plane.

RESULTS OF SIMULATIONS AND DISCUSSION

During the model crack growth cyclic stresses and strains around the crack front are almost stabilised. Therefore the results for the 39th cycle should simulate the behaviour of the crack of length a = 8.826 mm under given constant amplitude loading. All the results presented concern this idle cycle.

The results for 2D-plane stress simulation are demonstrated in Fig. 3. The cyclic behaviour of the crack in the thick wall is demonstrated by Fig. 4 (the central part of the front), by Fig. 5 (the corner point where the front intersects a free surface), and by Fig. 6 (at the depth $z = 0.028$ mm below the free surface). The left side of these figures shows the state at maximum loading, whereas the right side shows the situation after unloading. Vertical lines indicate the current crack front position. The following types of plots are presented: a) the crack profile in a plane parallel to the (x, y) plane b) total plastic strain distribution (ε_{xp}, ε_{yp}, ε_{zp}) in the x-direction c) the change of plastic strain ($\Delta\varepsilon_{xp}$, $\Delta\varepsilon_{yp}$, $\Delta\varepsilon_{zp}$) during the loading (on the left) and unloading (on the right) as a function of x; the x-dimension of the tensile (or compressive) plastic zone in (x,z) plane is thus visible d) stress distribution (σ_x, σ_y, σ_z) in the x-direction e) the x-distribution of the strain energy density increment $\Delta\lambda$ (or plastic strain energy density increment $\Delta\lambda_p$) during the loading cycle. Some vertical axis scales in Fig. 3 are different from scales in Figs. 4 - 6.

Plane stress solution (thin-walled body)
This solution corresponds to the behaviour of the crack in a very thin specimen. According to the well known Elber´s experimental relation $(P_{max} - P_{op})/(P_{max} - P_{min}) = 0.5 + 0.4\,R$ the crack opening load P_{op} for $R = 0.7$ is only 0.77 P_{max}. The model crack stays open during the whole cycle although the crack faces immediately behind the tip come very close (Fig. 3a).

The crack tip deformation mechanics can be characterised as follows: the low level of constraint indicated by the low level of the stress triaxiality, the high plastic strain range (Fig. 3c) together with the low absolute values of normal stresses (Fig. 3d), and the high strain energy density increment per cycle (Fig. 3e). The maximum shear stress induced by the maximum loading is high (342 MPa at a distance of 4 μm from the crack tip) and it acts on the planes that bisect the right angles between (x,z) and (x,y) planes. The maximum normal stress acts in the load direction and it is relatively low (684 MPa). Under such conditions the cyclic plastic deformation results in an intensive material damage and in elementary crack extensions in the slant plane of maximal shearing stress so that shear lips are formed.

The approximate theoretical estimation of the crack growth rate can be simply performed as follows. Let us assume an element A at the fatigue crack axis in front of the crack tip at some very small distance Δa. According to a modified critical strain-to-fracture model [9], the crack will extend to A during ΔN cycles satisfying the relation

$$\Delta\varepsilon_p\, \Delta N^{\beta} = \varepsilon_c\,. \tag{1}$$

Here $\Delta\varepsilon_p$ denotes the computed plastic strain range in the loading direction at point A during the loading cycle. The rate of simulated fatigue crack was estimated as $\Delta a/\Delta N \cong$ 0.10 μm/cycle.

Alternatively, according to Sih's energetic hypothesis [10], the crack is supposed to extend to point A after ΔN cycles, during which a critical amount λ_c of strain energy density is accumulated in A. The crack rate can be estimated as

$$\Delta a/\Delta N = (\Delta a\,.\,\Delta\lambda)\,/\,(\lambda_c - \lambda_m), \tag{2}$$

where $\Delta\lambda$ is the change of strain energy density in A during one loading cycle and λ_m denotes the mean value of λ in the cycle. Such theoretical model crack rate is $\Delta a/\Delta N \cong$ 0.11 μm/cycle.

The experimental crack rate determined from the effective stress intensity range [11] for a given material, loading, geometry, and a thickness of 5 mm is 0.07 μm/cycle. The surprising agreement between the experiment and the direct theoretical predictions should not be overestimated. However, the determination of parameters ε_c, β, λ_c from low-cycle fatigue tests with low level of constraint (uniaxial tension – compression) seems to be an important condition for obtaining good prediction from plane stress solution.

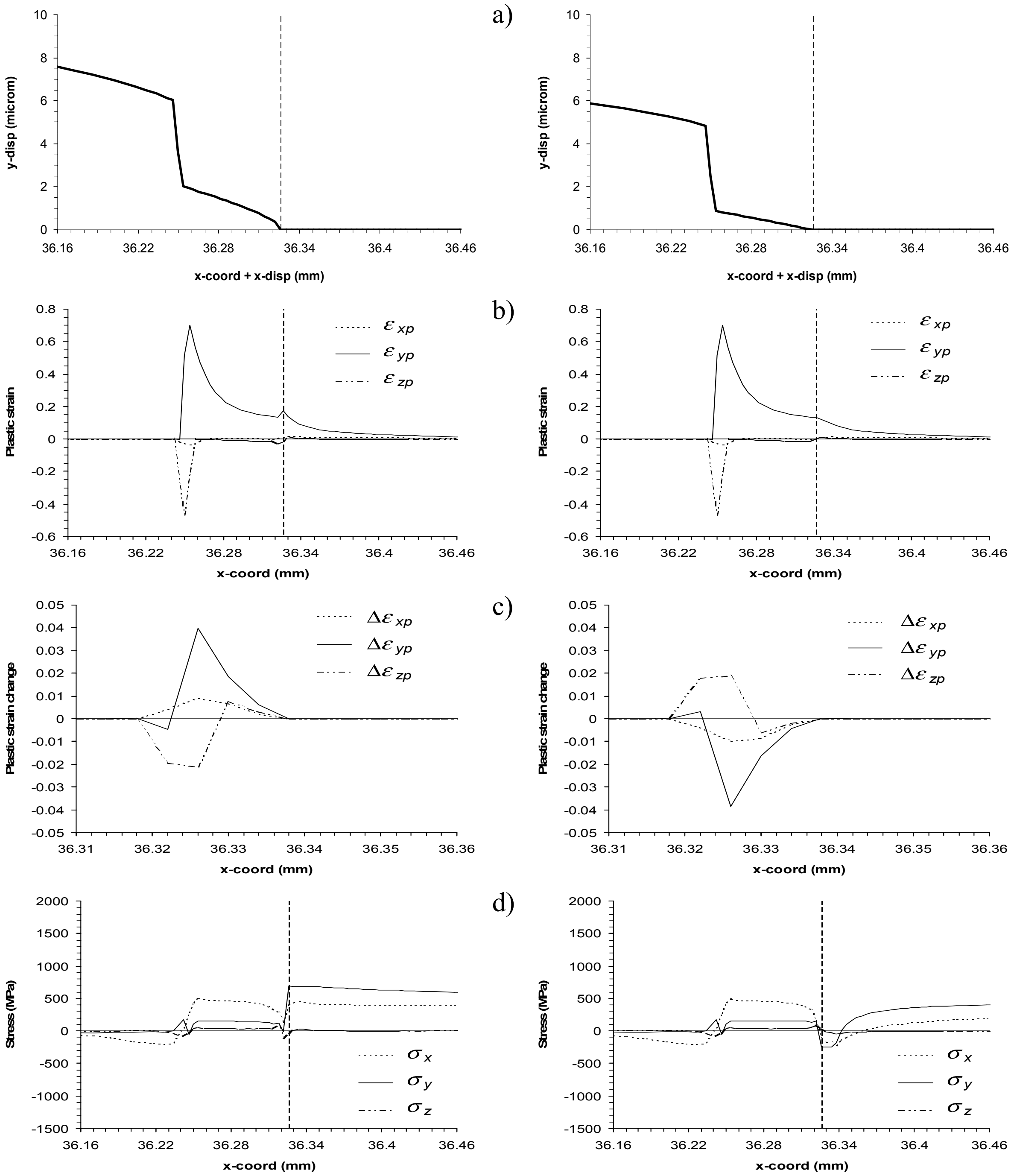

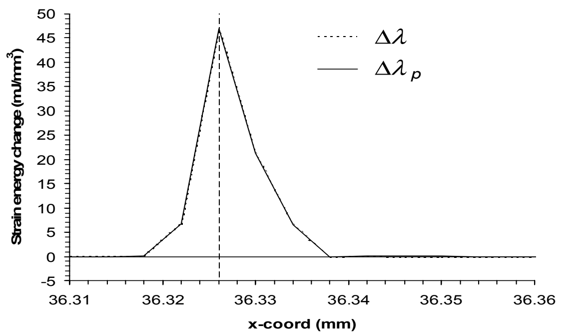

Fig. 3. Fatigue crack tip deformation mechanics resulting from 2D plane stress simulation.

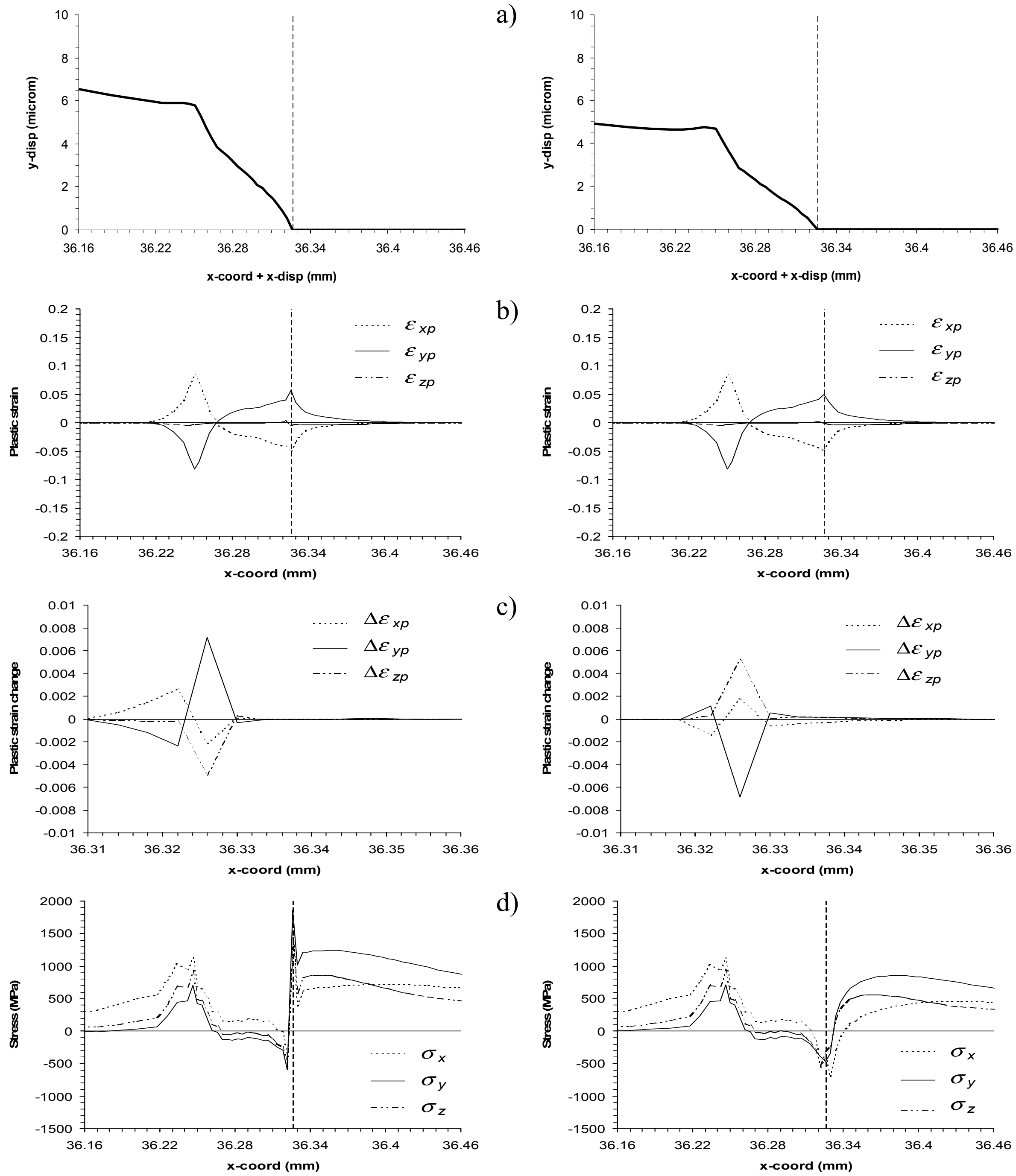

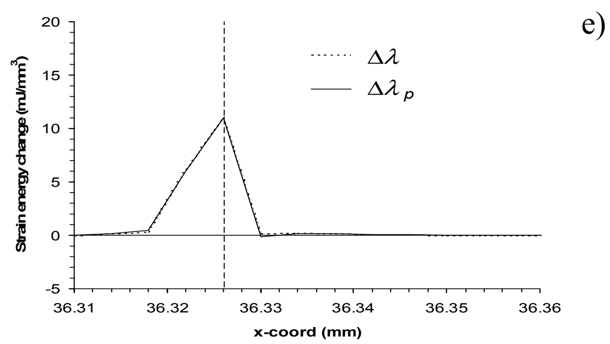

Fig. 4. Cyclic deformation at the centre part of the fatigue crack front (3D simulation).

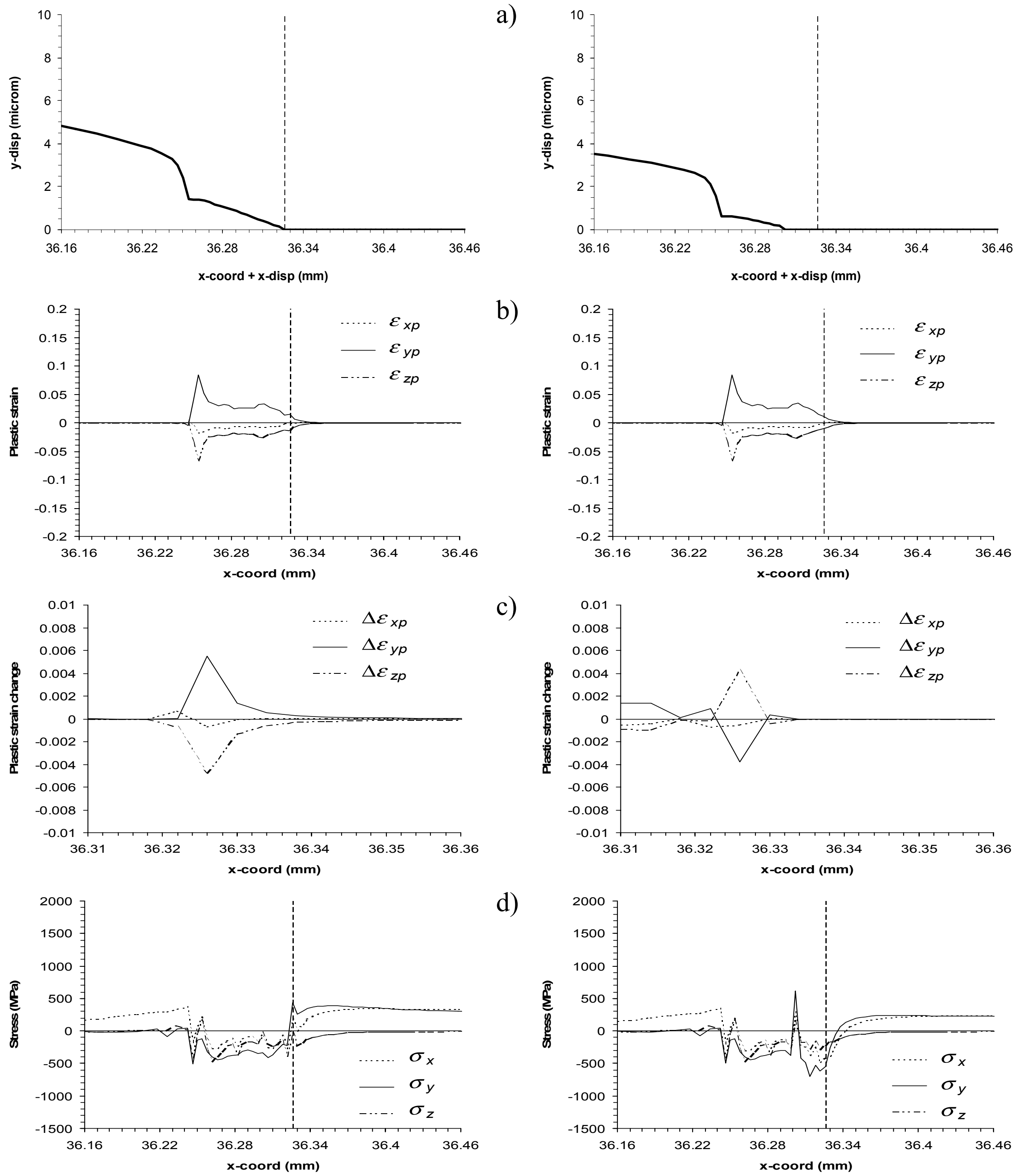

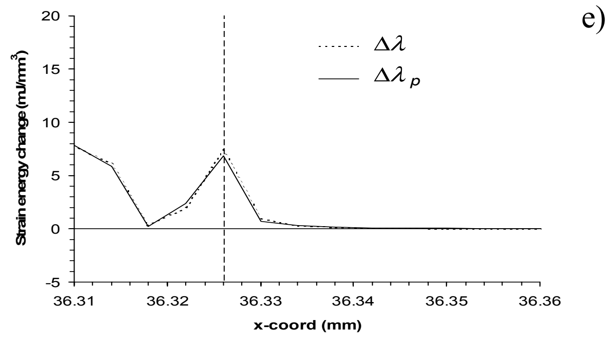

Fig. 5. Cyclic deformation at the end of the fatigue crack front (3D simulation).

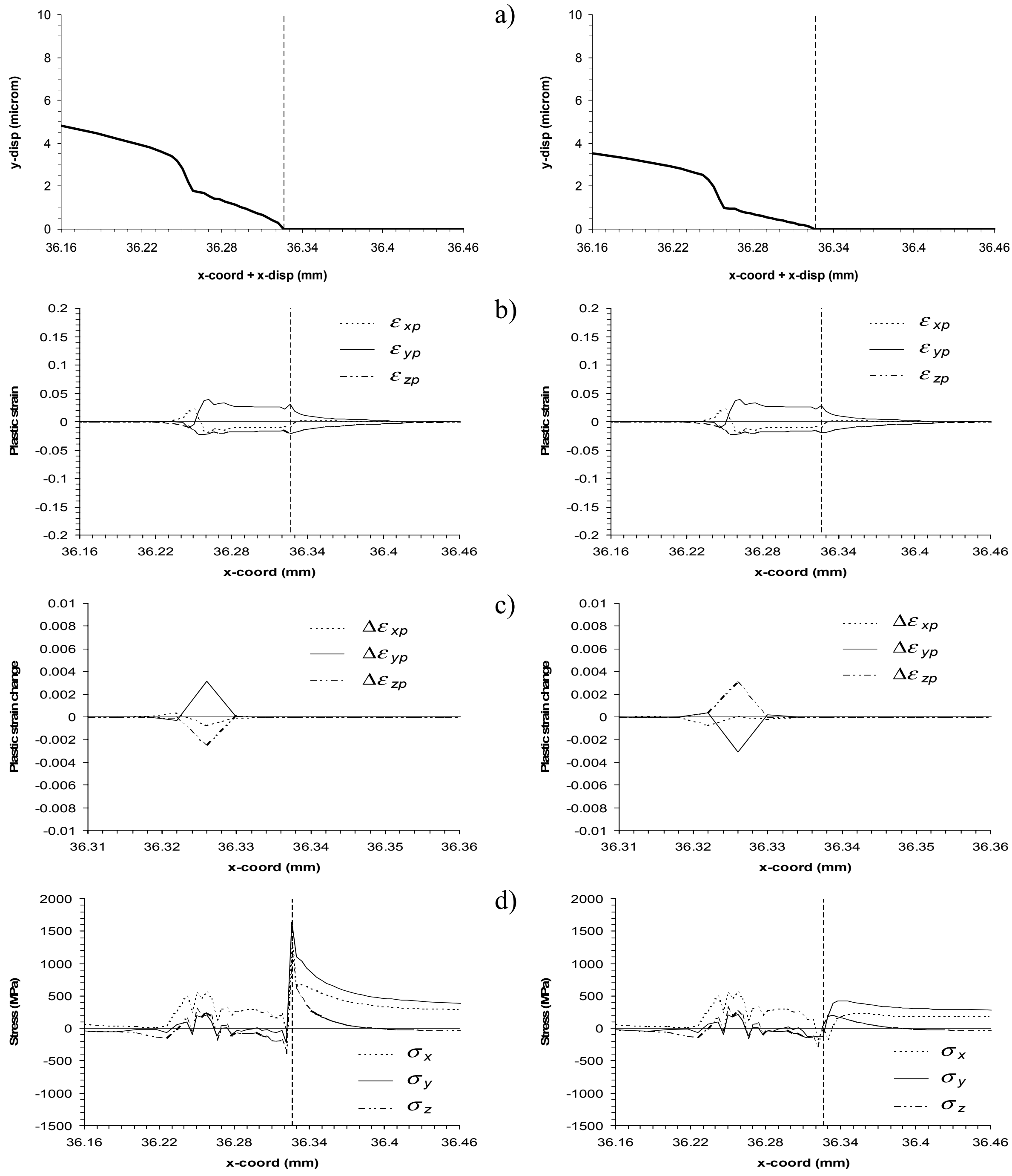

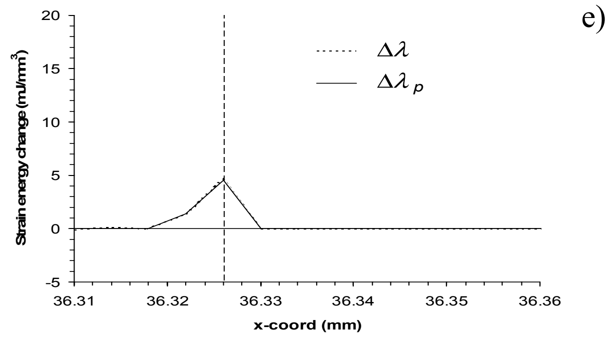

Fig. 6. Cyclic deformation at the fatigue crack front at the depth 0.028 mm bellow the free surface (3D simulation).

3D solution (thick-walled body)
Both the cyclic plastic deformation and the stresses immediately in front of the crack are practically the same for the whole crack front of the length 25 mm. The distribution of the plastic strain ε_{yp} and the distribution of the stress triaxiality indicating the level of constraint (the ratio of the mean stress and the von Misses effective stress) in the (*x, z*) plane are shown in Fig. 7. The influence of free surface extends no further than the very thin surface layer.

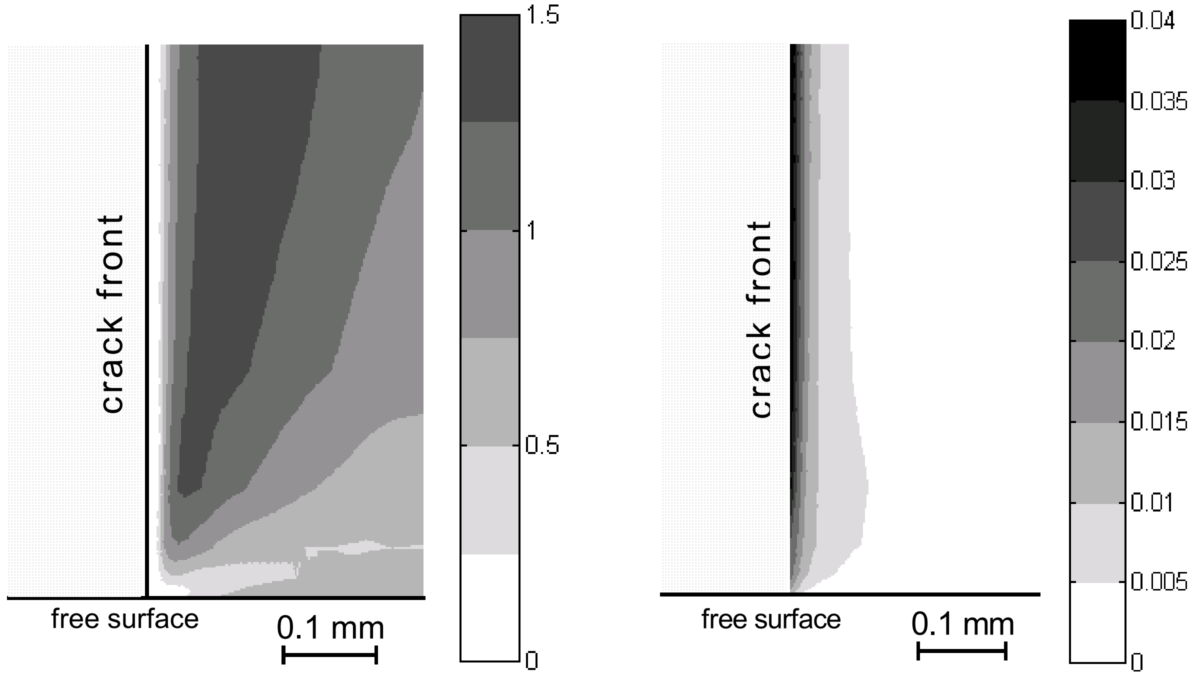

Fig. 7 Distribution of the stress triaxiality (left) and plastic strain ε_{yp} (right) near the intersect of the crack front with the free surface.

Residual plastic strains at fracture surfaces (immediately behind the front) in the vicinity of the corner of the crack are lower than in the centre (compare Figs. 5b, 6b with Fig. 4b). In spite of this, the crack margins at the free surface slightly close due to a local crack surface profile (Fig. 5a). However, the opening load for this closure is very close to $P_{min} = 0.7\ P_{max}$. The result is in good agreement with the known fact that the crack closing at a central part of the thick wall (Fig. 4a) is less intensive than the closing near the free surface (Fig. 5a, 6a). The overall picture corresponds also to direct ultrasonic measurements [1] that did not prove the closing of the real crack under such high stress ratio.

Initial tensile fatigue fracture mode (stimulated also by an aggressive environment) often changes into the shear mode so that shear lips appear on fracture surfaces. Through-thickness crack growth rate is usually not very much influenced by this transition nor does it very much depend on the thickness. Local stress conditions for a shear lips formation have not been quantified yet. Sometimes the visible transition to the shear mode can be preceded by a final fracture of a thick body. Such is the case of our CT specimen. The front of a real fatigue crack of the length $a \cong 8.8$ mm was macroscopically rectilinear, and the crack propagated in the tensile mode with an experimental rate of 0.08 μm/cycle [8].

Except for the thin layer at the free surface, the theoretical crack front deformation mechanics can be characterised as follows: low plastic strain range (compare Fig. 4c with Fig. 3c), very high normal stresses (compare Fig. 4d and 3d) resulting from a high level of the out-of-plane constraint, and relatively low strain energy density increment per cycle (compare Fig. 4e with Fig. 3e). The maximum shear stress acts on planes bisecting the angles between (x,z), and (y,z) planes and it is relatively low (314 MPa at a distance of 4 μm from the crack front), while both the stress triaxiality and the normal stresses are very high (maximum normal stress at the same distance is 997 MPa). The 3D results are roughly the same as the results of the 2D plane-strain simulation, including the fact that the cyclic plastic elongation to the loading direction is covered also by plastic contraction in the crack growth direction x (Fig. 4c).

The direct theoretical estimation of the crack growth rate could not be performed, because the low-cycle fatigue parameters for corresponding conditions were not available. The critical strain energy density for the high level of constraint is probably low. λ_c determined from the experimental crack rate and from the computed value of $\Delta\lambda$ is only a quarter of the value resulting from common fatigue tests under uniaxial loading. The high tensile stress seems to be sufficient for the elementary crack extensions even if the damage of the material by cyclic plastic deformation is not very intensive.

Three-dimensional results for the surface layer are quite interesting (the thickness of the layer in the thick CT specimen is only several tenth of mm) because they correspond neither to the plane strain nor to the plane stress simulation of the fatigue crack growth. The normal stresses and the stress triaxiality drop near the free surface and they are similar to the plane stress values (compare Fig.5d with Figs. 4d, 3d). However, the local cyclic plastic deformation (Figs. 5c, 6c) is restrainted both by nearby subsurface material and by crack closing. As a result, the plastic damage of the material as well as the local crack rate ought to be very low. However, if the surface part of the crack front lags behind the remaining part of the front, the strain range and the crack rate will increase again. Therefore a slightly curved shape of the stabilised crack front can be expected near the free surface. Such details were not been investigated in [8]. The real shape of the (slant) crack front and local conditions for the transition between the tensile and the shear fracture mode should be further studied and modelled.

CONCLUSIONS

A 3D elastic-plastic finite element simulation of the growing through-thickness planar fatigue crack with a straight front in a thick wall leads to the following main conclusions:

- Theoretical crack closing roughly corresponds to the available experimental results.
- Both the restraint against cyclic plastic deformation and high normal stress at a major part of the fatigue crack front in a thick wall are very similar to the corresponding 2D-plane strain simulation. A direct estimation of the crack rate from low-cycle fatigue conditions immediately before the front requires using of material parameters obtained from low-cycle fatigue tests at a high level of constraint. Critical strain energy density accumulated to fatigue fracture under such conditions should be substantially lower than the value resulting from common tests in tension-compression.

- The influence of the free surface extends only to a very thin surface layer. Three-dimensional results for the layer correspond neither to the plane strain simulation nor to the plane stress simulation of the fatigue crack. Low normal stresses are similar to the plane stress state, however, the size of plastic zones together with the low plastic strain range correspond rather to the plane strain simulation. At present the behaviour of end parts of the crack front cannot be theoretically predicted.
- 2D-plane stress simulation describes the situation only at the tip of the fatigue crack in a thin-walled body. A direct estimation of the crack growth rate based on the theoretical evaluation of low-cycle fatigue conditions at the crack tip and on the results of common low-cycle fatigue tests roughly corresponds to experimental results. The conclusions from [7] were thus confirmed again.
- For further improvement of fatigue crack growth simulations, several requirements should be pointed out: modelling of curved crack front, modelling of large strains, formulation of local conditions for the transition from the tensile fracture mode to the shear mode, improvement of damage cumulation model, and more detailed finite element solution.

ACKNOWLEDGEMENT

Financial support for this research by the Grant Agency of the Czech Republic, through grant No. 101/99/0384 "Finite Element Method in Nonlinear Continuum Mechanics and Application in Crack Propagation Problems", is gratefully acknowledged.

REFERENCES

[1] Materna A. and Oliva V.: *Acta Polytechnica* 40, (2000) 4.
[2] Oliva V. and Materna A.: In: *Engineering Mechanics 2000 –Vol. IV*. J. Náprstek, J. Münster (Eds.), Academy of Sciences of the Czech Republic, Prague, 2000, pp. 13-18.
[3] Newman J. C. Jr., Bigelow C. A. and Shivakumar, K. N.: *Engng Fract. Mech*. 46, (1993) 1.
[4] McClung R. C.: In: *Fatigue ´99*, X. R. Wu, Z. G. Wang (Eds.), HEP, Beijing, P. R. China, 1999, pp. 495- 502.
[5] Fissolo A., Le Roux L.C., Mottot M., Maillot V., Jayet-Gendrot S., Degallais S. and Francois D.: In: *13th European Conference on Fracture (ECF 13) - Fatigue*, Elsevier Science, San Sebastian, 2000.
[6] Oliva V. and Kuneš I.: In: *ASTM STP 1122*, M. R. Mitchell, R. W. Landgraf (Eds.), American Society for Testing and Materials, Philadelphia, 1993, pp. 72 -90.
[7] Oliva V., Cséplö L., Materna A. and Bláhová L.: *Materials Science and Engineering* A 234-236 (1997), pp. 517-520.
[8] Cerveny R.: Ph.D. Thesis, Ecole Centrale Paris, France, 1994.
[9] Davidson D. L. and Langford Jr. J.: In: *ASTM STP 811*, American Society for Testing and Materials, 1983, pp. 371-399.
[10] Sih G. C. and Moyer Jr. E. T.: *Engng Fract. Mech*., 17, (1983), pp. 269-280.
[11] Nedbal I., Siegel J., Kunz J. and Kopřiva P.: *Properties of Al-Alloy 7010*, Technical report V-KMAT –373/93. Czech Technical University - FNSPE, Prague, 1993.